Impact of functional group types in ion exchange resins on rare earth element recovery from treated acid mine waters

M. Hermassi [a,c,*], M. Granados [b], C. Valderrama [c], N. Skoglund [a], C. Ayora [d], J.L. Cortina [c,e]

[a] Thermochemical Energy Conversion Laboratory, Department of Applied Physics and Electronics, Umeå University, SE-90187, Umeå, Sweden
[b] Analytical Chemistry and Chemical Engineering Department, University of Barcelona, V. Diagonal 647, 08028, Barcelona, Spain
[c] Chemical Engineering Department, East Barcelona Engineering School, Barcelona TECHUPC, Eduard Maristany 10-14 (Campus Diagonal-Besòs), 08930, Sant Adrià de Besòs, Spain
[d] Institute of Environmental Assessment and Water Research (IDAEA-CSIC), Jordi Girona 18, 08034, Barcelona, Spain
[e] Water Technology Center CETaqua, Carretera d'Esplugues 75, 08940, Cornellà de Llobregat, Spain

ARTICLE INFO

ABSTRACT

Ion-exchange (IX) resins incorporating single functional groups (sulfonic or amino-phosphonic) and two functional groups (sulfonic and phosphonic) were evaluated for selective recovery of Rare Earth Elements (REEs) from acidic mine waters (AMW). The composition of AMW solution, complexing properties of the functional group, and acidity were investigated as key parameters for concentration and separation of REEs from transition elements (TEs). Fe has to be removed from AMW to enable REE recovery and here the AMW was treated with NaOH solutions to reach pH 3.9 where Fe(III) was selectively removed ($\leq$99%) by precipitation of schwertmannite. Single functional IX resin containing a sulfonic group displayed a higher REE recovery efficiency and separation ratio than observed for the bi-functional resin (sulfonic/phosphonic). Concentration factors for REEs between 30 and 40 were achieved using regeneration cycles with H_2SO_4. The performance of the amino-phosphonic resin showed lower separation factors for REEs from TEs than the two resins containing sulfonic groups. IX resins performance was improved by tuning the acidity to match the functional group reactivity, where pH adjustment to the range of 0.5–2.0 provided the highest REE/TE separation factor for the single sulfonic resin followed by the bifunctional resin. The integration of an elution cycle using Na_2-EDTA/NH_4Cl mixtures strongly increases the concentration factors of REE and Light REE (LREE) concentration factors of up to 260 were achieved for the single functional sulfonic resin.

1. Introduction

Rare Earth Elements (REEs) includes 15 lanthanides as well as yttrium and scandium, and have a common preferred electron configuration with preferred oxidation states of (+III). REE have been used in traditional sectors as metallurgy, petroleum, and textiles but are critical to several fast-growing high-tech industries such as electrical cars, clean energy technologies, batteries, superconductor materials, plasma televisions, and optical fibers (Chen, 2011; Xie et al., 2014; Zhang et al., 2017). They are considered as strategically important (Massari and Ruberti, 2013) and critical (COM, 2020; DOE, 2011; Zhang et al., 2020) raw materials. Five of them (yttrium, dysprosium, europium, neodymium, and terbium) are designated as critical rare earth elements (CREEs) by the U.S. Department of Energy (DOE, 2011) and the EU Commission

classification of critical raw materials (COM, 2020) since they are expected to be in short supply within the next two decades. Therefore, it is important to find new REE sources to meet the predicted growing demand that could exceed the world supply in less than a decade. The use of primary REE resources as well as REE-containing waste streams will likely be essential to meet this demand (Opare et al., 2021; Xie et al., 2014; Yang et al., 2013). In this context, exploration and identification of secondary REE resources and developing new processing technologies is necessary (Jha et al., 2016).

An example of secondary resource is acidic mine waters (AMW) where REEs have been found in concentrations up to 1000 times higher than those in natural waters (Noack et al., 2014). Such AMW can for example be found in the southern-west regions of Spain along main river basins such as the Odiel or Tinto basins, but can be found in various

---

locations globally. They are characterized by a low pH (1–3) and a large amount of dissolved metallic (e.g. Fe, Al, Cu, Zn) and non-metallic (e.g. As, Se) ions with REE in the mg/L concentration range (Nieto et al., 2013). AMWs represent a major sustainability challenge for the coal and metal mining industry due to their large volumes and the associated high treatment cost. AMWs are usually treated with lime or limestone to increase the pH and precipitate metal ions as hydroxides (Ayora et al., 2013). However, this strategy consumes large amounts of alkaline agents, and produces a water-rich sludge with a water content of 96–98% and a metallic content composed mainly of Fe and lesser amounts of Al, Zn and Cu, which together makes this processing option expensive.

New initiatives on sustainable mineral processing utilizing AMW as a mineral source may contribute to solving the environmental problem caused by AMW, as well as develop low-cost treatment options for utilizing AMW as a secondary resource for critical REEs (Ayora et al., 2016; Hedin et al., 2019; Stewart et al., 2017). As REE are present only at low concentration levels in AMW (mg/L range), such development of a recovery process should be focused on the selective and efficient extraction from the aqueous streams (Callura et al., 2021; Diallo et al., 2015; Papangelakis and Moldoveanu, 2014; Zhang and Honaker, 2018) for an economically viable treatment. Furthermore, recent studies provide a high-level assessment of the economic merits of recovering REE and select critical material from AMW sources using an innovative decentralized network supply chain configuration (Fritz et al., 2021; Larochelle et al., 2021).

Two strategies that could be used for REE recovery from AMW are solvent extraction (SX) (Sole, 2008) or ion exchange (IX) (Radhika et al., 2012; Xiong et al., 2012). A major challenge is effective separation of REE from transition elements (TE) that are typically present in AMW, especially Fe and Al. Therefore, recovering REE from secondary resources such as waste streams with SX requires selective extraction reagents or in the case of IX-resins and adsorbents selective resins (Xiong et al., 2009). A drawback with SX is the intense use of chemicals which could be reduced by introduction of IX technology. This strategy has proven successful in hydrometallurgical processing schemes as established SX processes in industrial scale plants were substituted by IX in the form of Resin in Pulp (RIP) (Quinn et al., 2015) and Resin in Leach (RIL) for gold (Syed, 2012), copper (Kuz'min and Kuz'min, 2014), and uranium (Mirjalili and Roshani, 2007). IX processes have been also postulated as a potential key technology to develop more sustainable processes for AMW management compared to traditional treatments (Reig et al., 2019; Simate and Ndlovu, 2014).

Recent work concentrated on different versatile sorbents for removing Rare Earth elements from aqueous medium using; phosphonate-functionalized composite, phosphorylated hydrogel (Algal Biomass/PEI) sorbent, magnetic Schiff's base chitosan composite, urea- and thiourea-based polymers (Hamza et al., 2022; He et al., 2021; Wei et al., 2021a, 2021b). Equally, recent groups have studied REE extraction from AMD, shown a higher affinity to optimize the recovery of REE from AMD precipitates by oxalic acid precipitation (Wang et al., 2022). Table S1 (supplementary Material).

Beside, previous intensive efforts have been allocated at research level to extend the types of IX functional groups in polymeric resins from the standard mono-functional strong acidic groups (e.g. sulfonic resins) or strong basic groups (e.g. quaternary ammonium resins) to weaker acid/base functional groups accompanied with coordinating groups (Littlejohn and Vaughan, 2012; Silva et al., 2018). Double-functional resins (e.g. di-phosphonic resins) or bi-functional resins (e.g. sulfonic-/phosphonic resins) (Reddy and Kumar, 2016) have been synthesized with the purpose of improving not only the selectivity factors and the regeneration cycles, but also to improve their kinetic performance.

Although IX resin performance has been improved by such multiple functionality, efforts to incorporate highly selective functional groups chemistry is associated with complex and expensive IXs resins that will likely only be used at preparative scale for analytical purposes. Less selective resins are therefore of higher relevance in REE recovery processes, where Izatt et al. (2014) (Izatt et al., 2014) and Page et al. (2017) (Page et al., 2017) studied the sorption properties of IX resins containing mixed sulfonic/phosphonic, aminophosphonic, and iminodiacetic acid functional groups to assist in the isolation of a mixed REE product with promising results.

In this work, mono-functional (sulfonic, aminophosphonic) and bi-functional (sulfonic/phosphonic) IX resins have been evaluated with respect to extraction and concentration of REE from AMW. The study aims to investigate the effect of acidity, amount of resin, or metal ion concentration on REE recovery using three IX resins with different functionality. The resins were investigated in batch and column experiments to study the equilibrium and extraction kinetics, with the best candidate resins further investigated using EDTA reagents for enhanced REE recovery.

2. Experimental methodology

2.1. Reagents materials and solutions

2.1.1. AMW sample preparation for batch and column sorption experiments

AMW samples were obtained from the abandoned mine of La Poderosa in the Odiel river basin (Huelva, Spain), with a pH between 2.2 and a high content of total Fe (1.7 g Fe/L). AMW raw samples and AMW after Fe removal, called Treated AMW (TAMW) hereon, were used for batch and column sorption experiments. Appropriate volumes of AMW were treated with an excess of H_2O_2 (5 times excess compared to the theoretical amount required to oxidize Fe) to oxidize Fe(II) to Fe(III) and then equilibrated overnight until the pH of the solution was kept constant. Then, controlled amounts of 4% (w/w) NaOH solution was added until the pH reached a value of 3.8 ± 0.2. It is expected that a near complete precipitation of Fe(III) and minimum removal of TE (Al(III), Zn (II), Cu(II)) and REEs occurs within this pH range (Lozano et al., 2020). Samples were kept in agitation for more than 24 h and finally filtered using quartz filters as described previously (López et al., 2021b). The pH was measured by using a combined pH electrode (Crison- GLP22) and was found to be in the pH range of 1–6 for all treated samples.

2.1.2. Ion exchange resins

IX resins used in the present work are Purolite SPC 11706 (sulfonic, abbreviated SPC11 from here on out), S950 (aminophosphonic), and S957 (sulfonic and phosphonic). All three are fixed in a cross-linked polystyrene (PS) divinylbenzene (DVB) macroporous matrix and their properties are provided as supplementary information in Table S2. Resins were provided by Purolite (Spain) in sodium form and were conditioned before use according to the method described by Reig et al. (2019) (Reig et al., 2019).
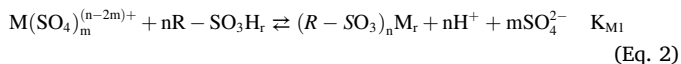
2.1.3. Formulation of metal extraction reactions for IX resins

2.1.3.1. Monofunctional sulfonic resin (SPC11).
The metal process extraction involves two steps according to i) and ii):

i) Dissociation reaction of the sulfonic group (R–SO₃H) (pKa = −0.6) as it is described by Eq. (1):

$$R - SO_3H_r \rightleftarrows R - SO_{3,r}^- + H^+ \quad K_{a(s)} \tag{Eq. 1}$$

ii) Metal extraction reaction as described by Eq. (2).

$$M(SO_4)_m^{(n-2m)+} + nR - SO_3H_r \rightleftarrows (R - SO_3)_n M_r + nH^+ + mSO_4^{2-} \quad K_{M1}$$

(Eq. 2)

where $R - SO_3H_r$ represents the sulfonic acid group of the IX resin.

2.1.3.2. Monofunctional aminophosphonic acid resin (S950). The metal extraction process involving an aminophosphonic functional group (R–NH–POOH$_r$) is a more complex system than for sulfonic resins due to
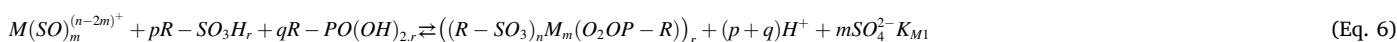
the presence of two functional groups, an internal secondary amine group (–NH–) and the terminal phosphonic acid group (-POOH$_r$) as it is described by Eq. (3):

$$HSO_4^- + R - NH - PO(OH)_{2,r} \rightleftarrows R - (NH_2^+ HSO_4^-) - PO(OH)_{2,r} \quad K_{NH3/HSO4}$$
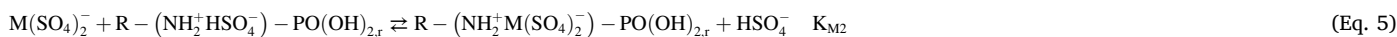
(Eq. 3)
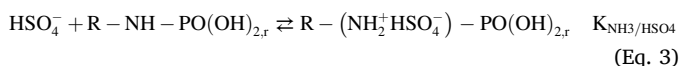
Where $R - NH_2 - PO(OH)_{2,r}$ represents the aminophosphonic group of the IX resin.

The aminophosphonic group is considered as a polyampholyte characterized by the presence of a secondary amine group between the styrene-divinylbenzene matrix and the phosphonic group. It can bind metal ions via oxygen atoms from the phosphonic group and via nitrogen atom from a secondary amine group. Phosphonic groups are moderately acidic and contain active centres of two kinds: phosphonic oxygen and hydroxyl acid groups and the sorption of REE/TE ions can proceed via their coordination interaction with the former, and through their ionic interaction with the latter. In most of the acidity range evaluated both the phosphonic and the secondary amine will be protonated as it is described by Eq. (4):

$$'M(SO_4)_m^{(n-2m)+} + nR - (NH_2^+ HSO_4^-) - PO(OH)_{2,r} \rightleftarrows (R - (NH_2^+ HSO_4^-) - POOO_2)_n M_r + nH^+ + mSO_4^{2-} \quad K_{M1}$$

(Eq. 4)

The metal extraction reaction describing the results observed for TE in strongly acidic solutions of sulfuric acid ([H_2SO_4]>0.5 M) involve an anion-exchange reaction with the protonated amine group (-$NH_2^+ HSO_4^-$) as described by Eq. (5):

$$M(SO_4)_2^- + R - (NH_2^+ HSO_4^-) - PO(OH)_{2,r} \rightleftarrows R - (NH_2^+ M(SO_4)_2^-) - PO(OH)_{2,r} + HSO_4^- \quad K_{M2}$$

(Eq. 5)

Metal extraction reactions involving anion exchange reactions postulated by Eq. (5) was proposed for S957 chelating resin but incorporating a methylene group between the aromatic ring of the styrene-divinylbenzene and the nitrogen atom of the amine (Kertman et al., 1995). From a regeneration point of view, metal complexes associated to the phosphonic acid group are bonded so strongly (KM1) that reversion

of the reaction by using strong acids is not favoured. Such metal complexes are formed in 10M H_2SO_4 solutions as observed in the present work (Supplementary material, Figure SM1).

2.1.3.3. Bifunctional sulfonic and phosphonic acid resin (S957). The metal extraction process will involve single reactions with both functional groups as described by Eq. (4) and Eq. (5), although it could not be discarded mixed metal-sulfonic-phosphonic complexes $((R - SO_3)_n M_m (OOP - R))_r$ as described by Eq. (6).

$$M(SO)_m^{(n-2m)+} + pR - SO_3H_r + qR - PO(OH)_{2,r} \rightleftarrows ((R - SO_3)_n M_m (O_2OP - R))_r + (p+q)H^+ + mSO_4^{2-} K_{M1}$$

(Eq. 6)

Regeneration of the resins should follow protocols supported on the reversion of the metal extraction processes described by Eq. (1) to Eq. (6).

2.1.4. Other reagents and chemicals

Analytical grade reagents were used to adjust pH of working solutions: NaOH (Merck), NH$_4$Cl (Merck), Ethylenediaminetetra-acetic disodium salt (EDTA) (Panreac) and H$_2$SO$_4$ (Sigma-Aldrich). H$_2$O$_2$ 30%(v/v) (Panreac) was used to oxidize Fe(II) to Fe(III) in acid mine water samples. All solutions were prepared using deionized Milli-Q (Merck-Millipore) water quality.

2.2. Batch equilibrium REE sorption experiments

Batch equilibrium sorption experiments were carried out using a standard methodology described by Reig et al. (2019) (Reig et al., 2019). Two different types of experiments were carried out as described below.

2.2.1. Effect of solid phase/aqueous phase solid ratio

Weighed amounts of dry resin samples (from 1 to 10 g) were shaken overnight with given volumes (50 mL) of TAMW at the natural pH conditions of each sample. After, for each tube, samples were centrifuged for 10 min and filtered (0.22 μm). The resin was separated by filtration and the pH of the solution was determined. The aqueous phase was analysed with ICP-AES/MS to determine resulting concentrations of REE and TE.

2.2.2. Effect of acidity on metal extraction

Weighed amounts of dry resin samples were shaken overnight with given volumes (15 mL) of TAMW at different acidity values with pH ranging from −1 to 5. Acidity was controlled by addition of 20% (w/w) H$_2$SO$_4$ or 4% (w/w) NaOH. All the experiments were carried out at room temperature (22±1 °C). After phase separation, pH was measured and

Table 1

Summary of the ion exchange column experiments (Col #) carried out with AMW from La Poderosa mine (Huelva, Spain) after Fe removal (TAMW).

Experiment	IX resin	Resin mass (g)	TAMW pH	1st Elution	2nd Elution
Col 1	SPC 11706	9.5	4.0	H$_2$SO$_4$ 10M	—
Col 2	S 950	9.5	4.0	H$_2$SO$_4$ 10M	—
Col 3	S 957	9.5	4.0	H$_2$SO$_4$ 10M	—
Col 4	SPC 11706	4.6	2.0	0.5 M Na$_2$EDTA + 1 M NH$_4$Cl	0.5M H$_2$SO$_4$
Col 5	S 957	3.6	2.0	0.5 M Na$_2$EDTA + 1 M NH$_4$Cl	0.5M H$_2$SO$_4$

metal ion concentrations were determined. For highly acidic solutions, defined here as pH < 1, acidity was determined by potentiometric titration with NaOH.

2.3. Kinetic REE extraction experiments

Kinetic extraction experiments were carried out using standard methodology described by Reig et al. (2019) (Reig et al., 2019). Weighed amounts of dry resins (1–10 g) were equilibrated with 100 mL of TAMW (pH 3.8 ± 0.2) in a 250 mL beaker. Liquid samples were withdrawn sequentially at given times from 1 min to 24 h. Samples were centrifuged for 10 min and filtered (0.22 μm) before analysis with ICP-AES/-MS to determine REE/TE concentrations. For the 24 h equilibration experiments the final pH was measured and if necessary adjusted to the initial pH values with NaOH/H$_2$SO$_4$ solution. REEs and TEs extraction percentage (E$_M$(%)) was calculated according to Eq. (7) based on the composition of aqueous solutions at the end of the experiments.

$$E_M(\%) = \frac{C_{M0} - C_{Me}}{C_{M0}} \times 100 \qquad \text{(Eq. 7)}$$

where C$_{Mo}$, and C$_{Me}$ are the initial and final total metal concentrations.

2.4. REE concentration and separation by ion exchange resins: column experiments

Two glass columns, 100 cm long and 1.5 cm in diameter, were filled with IX resins. A peristaltic pump (Minipuls 3, Gilson MP) was used to pump the different TAMW solutions through the column. A fraction collector (FC 204, Gilson) was used to collect effluent samples from columns. Specific conditions for the column experiments are listed in Table 1.

Columns were rinsed with water for 2 h at a flow rate of 1 mL/min previous to the experiments. Then, TAMW at pH = 4 (Col 1, 2, 3) and pH = 2 (Col 4, 5) was circulated at 1 mL/min through the column and samples were collected using a fraction collector. pH was adjusted to pH 1 for experiments Col 4 and Col 5 by using 0.5 M H$_2$SO$_4$. Finally, the elution of the metals sorbed was performed with a solution of 10M H$_2$SO$_4$, which was passed through the column at 0.25 mL/min. Collected samples from the sorption and elution experiments were analysed by ICP-AES/MS (see section 2.6) to determine the breakthrough curves and elution curves as a function of the treated bed volumes of TAMW or elution solution respectively. A two-stage sequential elution was carried out in experiments Col 4 and Col 5 as summarized in Table 1.

The breakthrough curves and elution curves were calculated as a function of the treated bed volumes of TAW or elution solution, respectively. The treated volume was expressed as Bed Volume (BV) defined by eq. (8):

$$BV = \frac{V_s}{V_b} \qquad \text{(Eq. 8)}$$

where V$_S$ is the treated volume and V$_b$ is the column pores volume determined from a tracer assay as described elsewhere (Crittenden et al., 2012; Reig et al., 2019).

2.5. Aqueous samples analytical techniques

AMW and TAMW were analysed with respect to their elemental concentrations for REE and TE. Measurement of pH was made with a Crison® glass electrode calibrated with buffer solutions of pH 7 and 4. Filtered samples (0.22 μm) were acidified with HNO$_3$ for analysis of major and trace elements. Major cations (Mg, Ca, Fe, Mn, Zn, Al) and total S were measured by ICP-AES (PerkinElmer® Optima 3200 RL) and trace metals (Cd, Co, Cu, Ni, Pb) with ICP-MS (PerkinElmer® Sciex Elan 6000). Detection limits were 0.1 mg/L for S; 0.05 mg/L for Mg, Ca; 0.02 mg/L for Fe, Mn, Zn; 5 μg/L for Al; 1.5 μg/L for Ni, Cu; 0.5 μg/L for Pb; and 0.2 μg/L for Co, Cd and REE. The analytical precision error was calculated as approximately 6% for ICP-AES and 5% for ICP-MS measurements.

3. Results and discussion

3.1. Characterization of the AMW and removal of Fe(II)/Fe(III)

The composition of AMW from the Poderosa mine is summarized in Table 2. The concentration of REE ranged from 0.01 mg/L for Lu up to 3.3 mg/L for Ce. Three main groups could be defined according to the concentration: i) 0.5–3.3 mg/L (Gd, La, Y, Nd, Ce); ii) 0.1–0.5 mg/L (Yb, Er, Hf, Dy, Pr, Sm) and iii) 0.01–0.1 mg/L (Lu, Tm, Ho, Eu). The low concentrations observed for Lu and Tm led to their exclusion from further analysis. In the case of TE the highest concentrations was
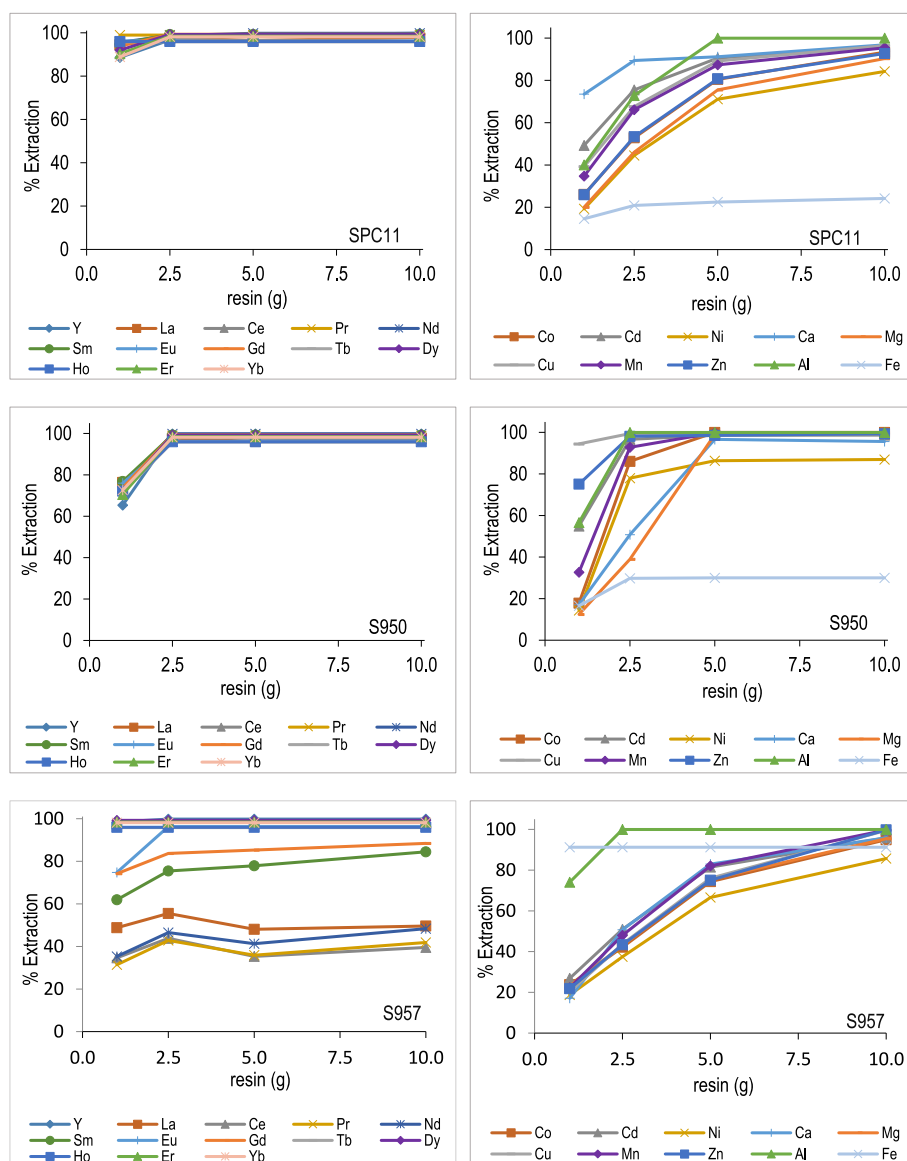
Table 2

Light Rare Earth Elements (LREE), Heavy Rare Earth Elements (HREE) and TE concentration (mg/L) in the raw AMW sample and after Fe removal treatment (TAMW) including the resulting removal percentage (R%). Only the most relevant TE and REE are shown.

Rare Earth Elements (REEs)						Transition metals (TEs)				
REEs		AMW (mg/L)	TAMW (mg/L)	R (%)		TEs	AMW (mg/L)	TAMW (mg/L)	R (%)	
LREE	La	1.13	1.00	11.5		Co	1.31	1.21	7.6	
	Ce	3.03	2.57	15.2		Cd	0.39	0.36	7.7	
	Pr	0.41	0.35	14.6		Ni	0.26	0.28	0.0	
	Nd	1.77	1.55	12.4		Ca	145.5	137.2	5.7	
	Sm	0.48	0.41	14.6		Mg	163.9	148.4	9.5	
	Eu	0.07	0.06	14.3		Cu	106.5	86.4	18.9	
	Gd	0.5	0.43	14.0		Mn	8.7	8.3	4.6	
HREE	Tb	0.08	0.07	12.5		Zn	95.2	87.2	8.4	
	Dy	0.37	0.32	13.5		Al	373.9	234.7	1.3	
	Ho	0.06	0.052	13.3		Fe	1588.9	7.3	99.5	
	Er	0.14	0.12	14.3		—	—	—	—	
	Yb	0.09	0.08	11.1		—	—	—	—	
	Y	1.62	1.47	9.3		—	—	—	—	

Fig. 1. REE and TE extraction (%) for TAMW (10 mL), at pH 3.8, as a function of resin weight (g) for SPC11, S950, and S957 resins.

observed for Fe with up to 1.5 g Fe/L, followed by a group of elements between 100 and 380 mg/L (Al, Mg, Ca, Cu and Zn) and a group of elements below 2 mg/L (Co, Ni, Cd among others). It is worth to mention that Al displays a similar chemistry to REE (Lozano et al., 2019) making it necessary to reduce its presence in the TAMW.

Table 2 summarizes the removal percentage (R (%)) of TE and REE after the oxidation of Fe(II) to Fe(III) and the alkaline treatment of the AMW by NaOH (TAMW). Losses of the REEs of highest concentration are below 15%. Pre-treatment provided Fe removal ratios up to 99%, however, only <2% of Al was removed. NaOH treatment was used to adjust AMW pH in the range of ~3.8 where removal of Fe(III) occurred by schwertmannite ($Fe_8O_8(OH)_6SO_4$) precipitation.

Analysis of the brown to orange colour sludge obtained by SEM-EDS and XRD identified the presence of schwertmannite. However, it could not be discarded the formation of amorphous ferric oxy-hydroxide by its formation occurs at pH > 5.5 (Bigham et al., 1996). It should be mentioned that previous experience and efforts of some of the authors were devoted on treatment of acidic waters influencing natural water bodies from abandoned mines (Ayora et al., 2013). Results of these studies indicated the formation of amorphous Fe (III) mineral phases containing sulfate ions (e.g. schwertmannite), especially in AMW with

large content of sulphates (>10 g/L) and if pH is kept below 5.5 as it is the case of the used in this study.

Similar results were reported by Ayora et al. (2016) in industrial scale treatment of several AMWs (Ayora et al., 2016). When analysing the REE behaviour, removal ratios were below 5% at this pH. Al can be removed by precipitation of basaluminite if pH is adjusted to values above 4 using NaOH addition, but practically all REE will then be retained in the basaluminite layer formed (Lozano et al., 2020).

The REE separation process should, based on these observations, attempt to achieve the maximum Fe(III) removal with minimal losses of REE included in basaluminate. Therefore, it is proposed to treat AMW with alkali to adjust its pH to 3.9 – this causes Fe compounds to precipitate while retaining both Al and REE in the TAMW formed, which aligns with other experiences reported previously in environmental studies on AMW treatment (Hermassi et al., 2021a, b).

3.2. Equilibrium and kinetic performance of IX resins (SPC11, S950, S957)

Preliminary extraction performance of REE and TE were carried out as a function of the resin weight (Fig. 1). In general, REE extraction was
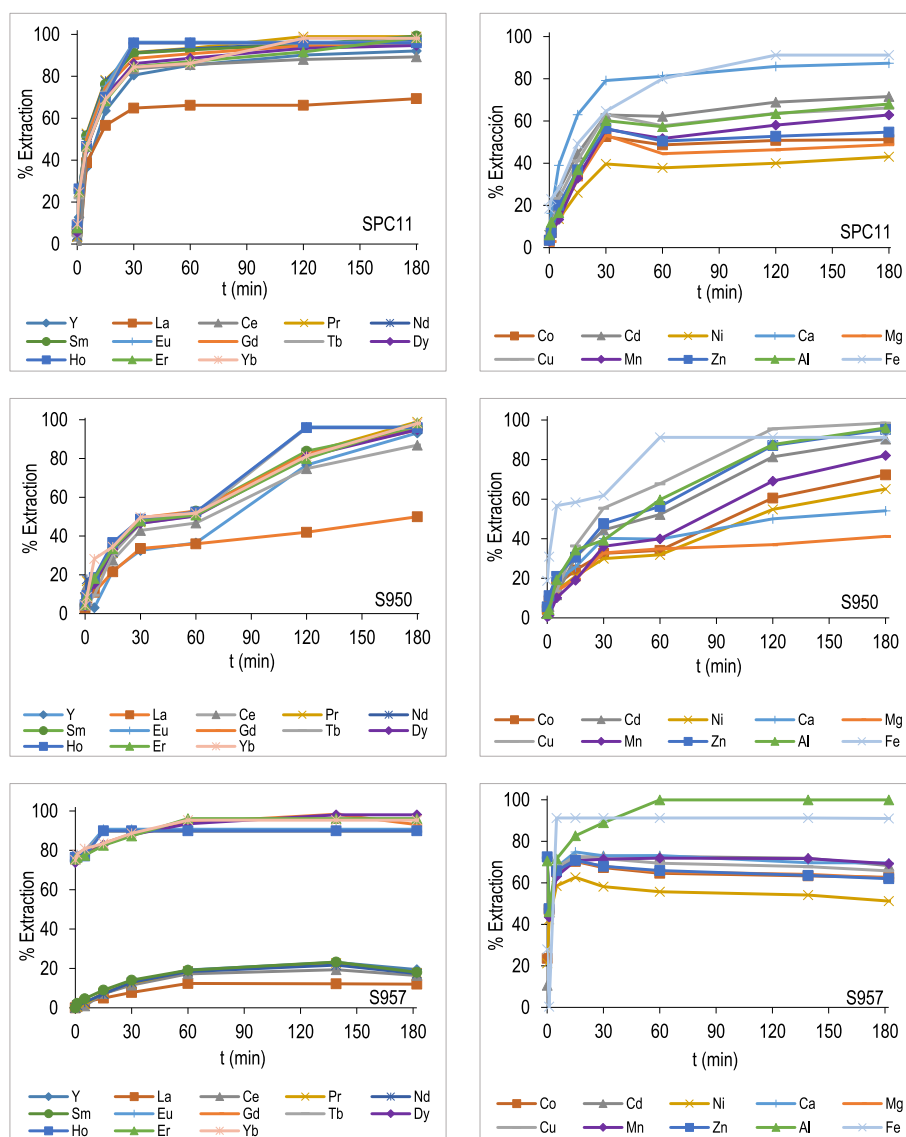
Fig. 2. Variation of REEs and TEs extraction ratio %E(t) as a function of time for SPC11, S950 and S957 resins for TAMW at pH 3.9 (S/L ratio: 5g/100 mL).

favoured over TE ions at the lowest ratio of resin to solution (mass/volume), especially compared to TE in form of divalent metal ions for the three IX resins. No significant selectivity was identified between the REE groups for the sulfonic (SPC11) or the aminophosphonic (S950) resins and they both displayed higher sorption performance than S957. The bi-functional resin S957 displayed a higher extraction efficiency for HREE than LREE.

Such extraction pattern is driven by the coordination properties of the phosphonic and sulfonic functional groups. This behaviour was not shown by the aminophosphonic group of the resin S950 despite that similar acid-base properties for both the phosphonic and the amino-phosphonic acid groups were expected. Similar results on separation patterns have been reported for impregnated resins containing the organophosphonic di-trimethyl-pentyl phosphonic acid when used to recover REEs from AMWs at pH 4 with HREEs preferentially extracted in front of LREEs (Hermassi et al., 2021a).

For TEs, mono-functional resins (SPC11 and S950) did not provide high extraction performance for the residual levels of Fe(III), while the bi-functional IX resin extracted both Fe and Al at similar efficiencies. This high selectivity for Fe(III) has previously been reported (McKevitt, B. and Dreisinger, D., 2009; McKevitt, Bethan and Dreisinger, David, 2009) when bi-functional resins were applied for removal of Fe(III) from

Cu tank house electrolytes in the cupper industry. In stoichiometric ratio of metals to total exchange capacity, REEs are preferentially extracted over TEs.

The variation of the pH along the metal exchange reactions as a function of the solid/aqueous phase ratio is shown in Table S3 (supplementary material). For the two mono-functional resins (e.g. SPC11 and S950) the measured equilibrium pH values were quite constant independently of the amount of resin and only for the case of S597 the pH decreased as the amount of resin increases. The decrease of the pH for S957 was due to the fact that total conversion to the sodium form was not possible. Then, the acidity of the resin is higher and this was traduced in the increase of the solution due to the exchange of metals to the resin phase.

The results of the kinetic performance at an initial pH 3.9 are depicted in Fig. 2 SPC11 showed a typical contact time for extraction where equilibrium attainment (>90% extraction) was reached in between 15 and 30 min. However, for the case of the phosphonic resins S950 and S957 (mono- and bi-functional) equilibrium was only achieved after between 30 and 45 min. This behaviour was observed for both REEs and TEs.

S950 shows a two stages time kinetic profile with a first plateau around 30–45 min and a second of more than 180 min before

equilibrium attainment. These long equilibrium attainment times were associated to the limited buffering capacity of the phosphonic acid resin, in comparison with the sulfonic resins. Both sulfonic containing resins (SPC11 and S957) showed a higher capacity to buffer pH along the long kinetic tests, especially in high acidic solutions (Fig. 2). In the case of S950, with weaker acidic groups (e.g., only phosphonic group) the typical S-shape function appeared after the 15–30 min, with an increase of the extraction rate which stabilizes after 60 min. This trend is correlated with an increase of the solution pH that favours extraction of REE over TE. Page et al. (2017) (Page et al., 2017) have previously shown that strong acidic resins with sulfonic functional groups display a high adsorption strength for the REE, high exchange capacity, fast exchange kinetics, as well as a high selectivity over monovalent and divalent cation impurities.

The variation of the pH along the metal exchange reactions is shown in Figure SM2 (supplementary material). As it could be seen the change of pH was driven by the excess of resin used in the kinetic experiments. For the two mono-functional resins (e.g. SPC11 and S950) the pH almost was constant along the equilibration time and only for S950 a small increase was measure due to the remaining excess of alkali in the resin after the conversion to the sodium form. In the case of the bi-functional resin S957, as the total conversion to the sodium form was not possible

and then the pH decreases due to the exchange of proton ions due to the metal extraction reactions. As the variation of pH is affecting the metal extraction reactions its value should monitored in the column operation as will be shown in the next section.

The lower kinetic performance of S950, with weaker acidic groups (e.g., only phosphonic group) will imply the need to increase the residence time of the TAMW in the bed column to assure at least equilibrium attainment higher than 90%.

3.3. Separation of REEs from TEs: identification of the acidity operation range

Separation factors of metal ions with IX resins are strongly controlled by: i) the acidity of the solution; ii) the presence of inorganic complexing anions in solution; and iii) the acid-base properties of the resin (pK$_a$ of the functional groups) (Jha et al., 2016; Silva et al., 2018). The presence of complexing anions and acidity influences the complexation in solution of the metal ions. As AMW are rich solutions on sulfate ions, sulfuric acid was used to adjust the acidity of the solutions and then both REEs and TEs (M^{3+}/M^{2+}) are partially complexed with SO_4^{2-} ions forming MSO_4^+/MSO_4 typically and in some cases, could be present as $M(SO_4)_2^-/M(SO_4)_2^{2-}$. This was investigated by a thermodynamic
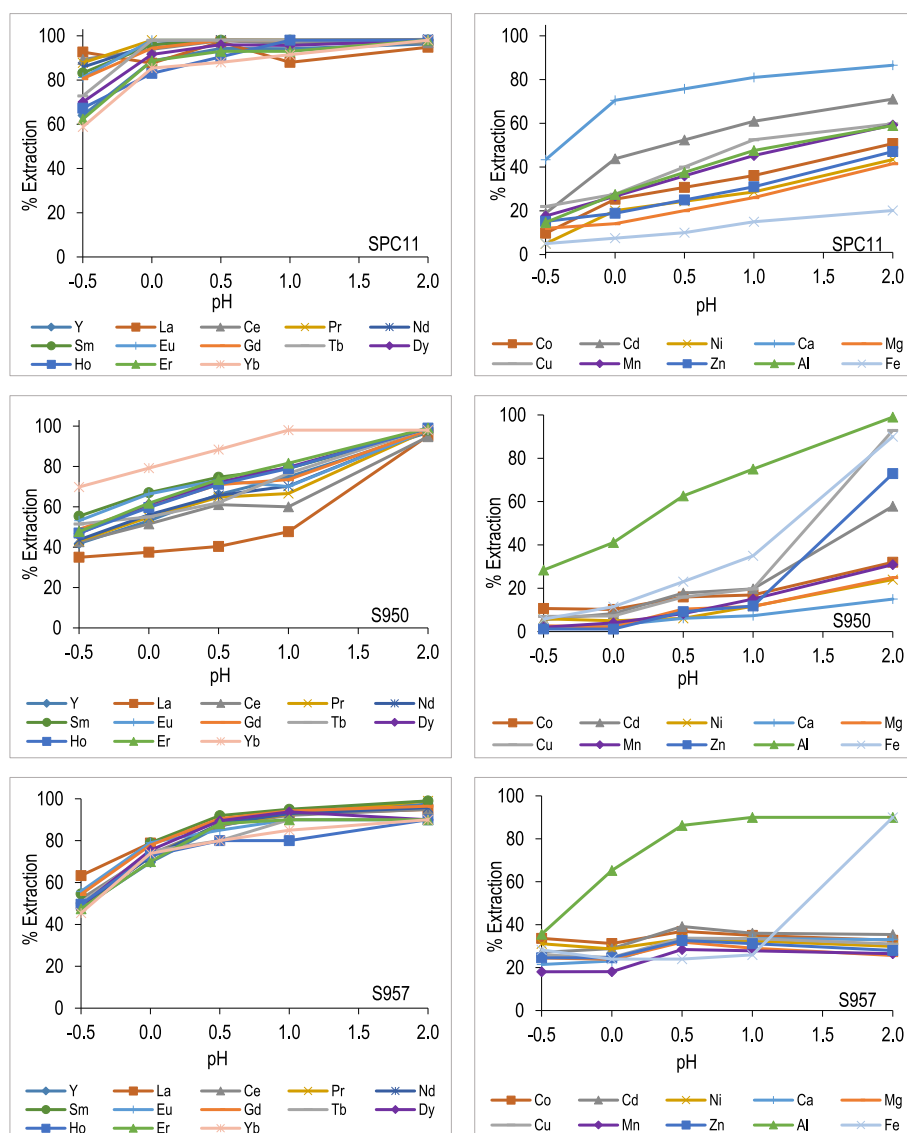

Fig. 3. Variation of the extraction percentage of REE and TE from TAMW using SPC11, S950 and S957 resins. S/L = 2 g of resin/50 mL of TAMW.
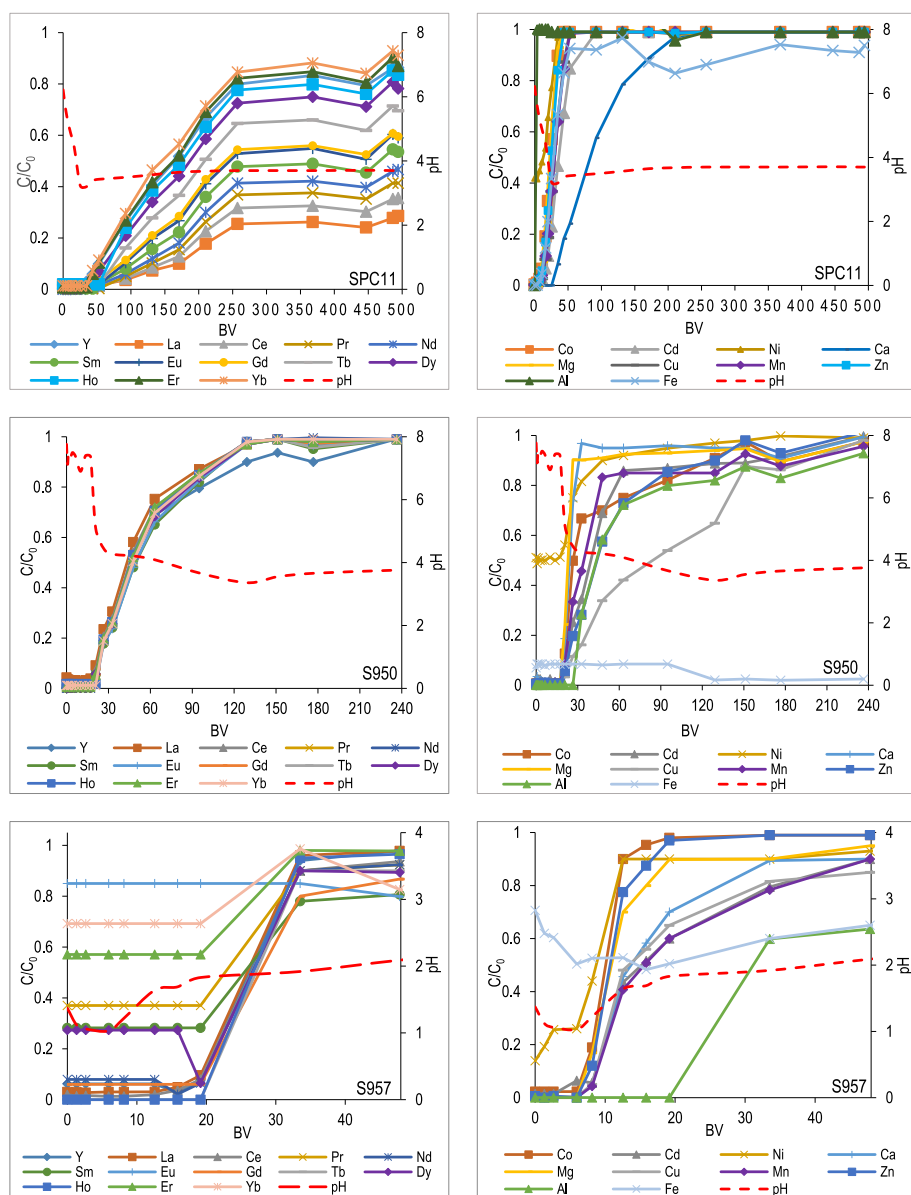
Fig. 4. Breakthrough curves (C/C$_0$) of (a, c, e) REEs and (b, d, f) TEs and the evolution in acidity of the column effluent as a function of the TAMW solution in BV (dashed line) for resins SPC11, S950 and S957 respectively.

equilibrium speciation study of REEs/TEs, a summary is available in Figure SM1 (Supplementary material).

As can be seen in Fig. 3, using a fixed adsorbent concentration S/L (TAMW) (2g/50 mL) and varying the initial pH window (−0.5 to 2.0), the extraction of REE occurred at more acidic conditions than TE extraction for all three IX resins investigated. Resins containing sulfonic functional groups (SPC11 and S957) were more efficient for REE extraction than the monofunctional phosphonic resin (S950) that does not display REE extraction efficiencies over 90% until pH = 2.0. It is worth to mention that TE final extraction by the sulfonic resin (SPC11) is 20% lower than observed for the bifunctional resin (S957) along the acidity range evaluated but similar trends of REE extraction is observed for both mono- and bifunctional resins at low acidity.

Page et al. (2017) (Page et al., 2017) evaluated three IX resins (bifunctional sulfonic/phosphonic, aminophosphonic and iminodiacetic) to separate La, Sm and Ho from Al, Fe and Th in sulfuric acid media. The IX resins displayed a similar selectivity for Fe and Th that were sorbed in preference to the REE and Al (i.e. Th ≃ Fe ≫ REE ≃ Al). Their results are comparable to those reported here and further confirm

that it is necessary to remove Fe(III) from TAMW to avoid a reduction of resin efficiency.

According to section 3.3, the highest recovery ratios for REE could be achieved at the acidity-window pH (0.5–2.0) (Fig. 3). Then samples of AMW after Fe removal (TAMW composition on Table 1) with pH > 0.5 were used without any modification of the pH.

3.4. Recovery and concentration of REEs from TAMW by using column experiments

3.4.1. Recovery of REEs from TAMW

Fig. 4 summarise the breakthrough curves (C/C$_0$) and the variation in acidity throughout the column using resins SPC11, S950 and S957, respectively.

As shown in Fig. 4, the REE breakthrough points for SPC11 started between at 35 BV for HREE and then followed by the LREE at 50 BV, indicating the higher selectivity of SPC11 for LREE over HREE at the acidity conditions used (described in section 2.4). When analysing the performance of the SPC11 resin with TE, trivalent and divalent elements
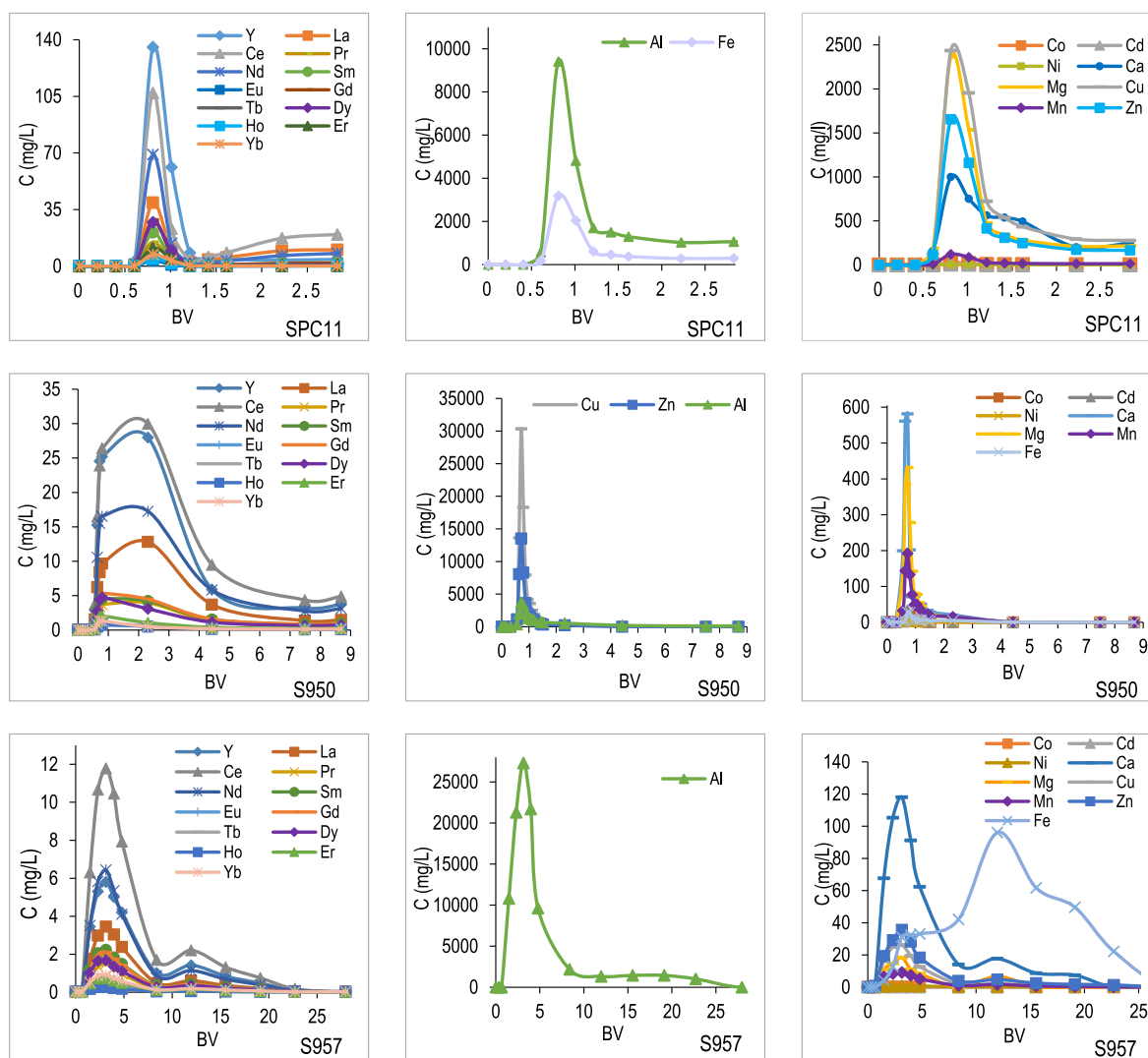
Fig. 5. Elution curves showing the variation of the metal ions concentrations: a) REEs and b) TEs (Al) and c) TEs (Fe, Co, Cd, Cu, Ni, Zn, Ca, Mg, Mn) as a function of the elution solution (10 M H_2SO_4 solution) in BV for resins SPC11, S950 and S957 respectively.

have shorter breakthrough values (below 20), the only exception was Ca with a behaviour similar to REE. The selectivity sequence on weaker K_M values were Ni < Co < Cu < Zn < Cd < Mn. Similar results with a strong acidic resin was reported by Ang et al. (2017) (Ang et al., 2017) when they studied extraction of REE from sulfate solutions.

Values of 20 BV for TE and 30 BV for REE are the short breakthrough points ($C/C_0 = 0.1$) for S950. The chelating aminophosphonic resin is showing a small difference affinity between of REEs and TE. The aminophosphonic chelating resin showed a limited capacity for separation of TEs from REEs as only small affinity differences could be observed.

In the case S957 resin, HREE (Dy, Ho, Er, Yb) and Eu and Pr were only partially sorbed with C/C_0 values between 0.3 and 0.9, whereas LREE were removed efficiently before reaching the breakthrough around 20–25 BV. Similar behaviour of partial removal was observed for Fe(III), while divalent TE showed a shorter breakthrough of 10 BV. A higher affinity pattern was observed for Al(III) with the largest breakthrough and with a similar pattern shown by LREEs. The strong affinity of REE with the sulfonic group is sufficient for recovery and no differences between sulfonic-containing resins (SPC11 and S957) were found.

3.4.2. Concentration of REEs from TAMW by using elution column experiments

Results on elution performance of the column after treating 500, 235

and 50 BV using a 10 M H_2SO_4 for resins SPC11, S950 and S957 respectively are shown in Fig. 5. Elution profile for SPC11 resin, the TE show sharp peaks indicating the efficiency of the elution step, with more than 95% were eluted in less 1 BV. Similar elution performance was reached for trivalent TE (Fe, Al) and also for Ca, Mg, Zn and Cu long tails were observed.

Although the concentration factors depend on the operation threshold but for a breakthrough point of 10%, the concentration factors were up-to 70 for most of the REEs. Total REE content on the elution solution were around 0.3 g REE/L. Moreover, results on elution performance of the column for S950, elution profile of TE show sharp peaks with more than 95% eluted including trivalent elements (Fe(III) and Al (III)) in less 1 BV. Elution peaks for REE separation with S950 resin (Fig. 5) display a broad breakthrough curve with most REE observed in the BV range from 0.5 to 5. Quantitative recovery of REE (<80%) was reached after 8 BV and (<70%) in 5 BV. This limits the application of aminophosphonic resins for concentration purposes of REE from AMW. For that reason, the S950 resin was excluded in the following section using other complexing reagents as Na_2-EDTA.

Elution using S957 resin showed short breakthrough values that were accompanied with wider elution peaks of 6–7 BV for REEs and TEs including also a small double peak as it is shown in Fig. 5. Quantitative recovery of REE (>95%) was reached after 10 BV with a 90% recovery
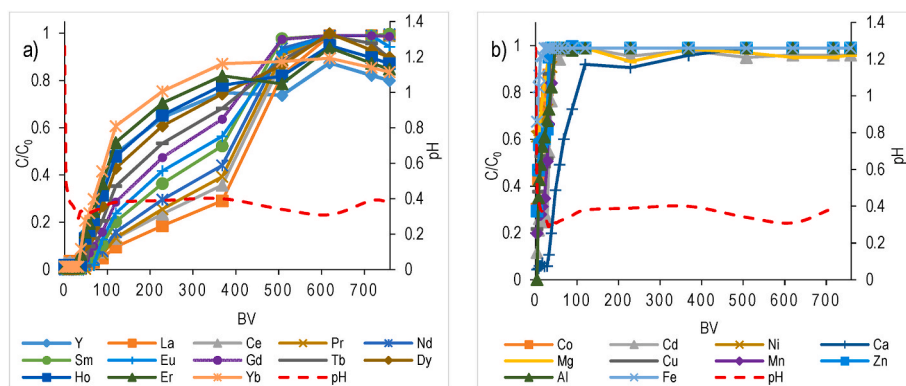
Fig. 6. Breakthrough curves for the extraction of a) REE and b) TE from TAMW conditioned at pH 2.0 as a function of treated water (BV) for SPC11 resin.

reached in 8 BV.

Although phosphonic groups have shown good performance on REE extraction and processing in solvent extraction circuits, when functionalized in resins their selectivity decreases and their kinetic performance is not comparable to that of sulfonic resins. In general, the concentration factors for REEs reached values below 2–3, it can be due to the strong metal-phosphonic complexes (K_M) and a limited selectivity factor respect to TEs. Thus, the use of S957, is limited to recover REEs, or increasing the acidity of the TAMW to increase the selectivity factor associated to the sulfonic group. Hence, it can be concluded that, in the tested conditions, the bifunctional exchanger is not suitable for REEs recovery and separation from TEs from TAMW and is not suitable to reach high concentration factors using an elution cycle via acidic regeneration with H_2SO_4. The potential regeneration with complexing reagents such as Na_2-EDTA is further explored for resins with sulfonic functional groups in section 3.5.

It should be mentioned the higher performance of SPC11 on the regeneration of RRE, transition elements and post-transition elements as Al(III) with short bed-volumes of H_2SO_4 solutions (e.g. 1–3 BV) when compared with S950 and S957 resins. Both chelating resin reported higher needs of H_2SO_4 for regeneration (3–5 BV) of REE and it should be mentioned that in the case of S957 with two functional groups two elution peaks were observed. The presence of these two peaks could be associated to the presence of the two different functional groups in the resins. Similar behaviour was observed for S957 for transition elements and post-transition elements (e.g. Al(III)).

3.5. Optimization of the recovery of REEs by acidity control and elution with complexing reagents

3.5.1. Concentration of REE with SPC11 using TAMW acidified at pH 2.0

According to results on section 3.3, the maximum recovery ratios for REE could be achieved at acidity-window pH (0.5–2.0) (Fig. 3),

therefore samples of TAMW were treated to reach pH = 2. Breakthrough curves for REE are shown in Fig. 6, where breakthrough values were from 40 BV for Yb up to 150 BV for La, using a breakthrough point of 10%. For the case of La(III) until 350 BV only values of C/C_0 of 0.3 was reached, after that higher number of 0.8 from 510 BV determined.

The breakthrough points or REE started between at 20–25 BV for HREE and then followed by the LREE at 35–40 BV (Fig. 6a), indicating the higher selectivity of SPC11 for LREE over HREE. At the acidity conditions used, TE were not retained with the only exception of Ca which was partially sorbed with a breakthrough point at 28 BV. The pH values at the column effluent were around 0.4, due to the exchange of protonated sulfonic groups with the REE. Page et al. (2019) (Page et al., 2019) reported that an increase of sulfate concentration promoted a reduced selectivity for REE when using a similar sulfonic resin. In this study, the increase of sulfate concentration due to the addition of sulfuric acid was not affecting the REE selectivity.

Elution of the loaded resin after treating 750 BV was carried out using 0.5M Na_2-EDTA and 1M NH_4Cl solutions and the elution curves for REE and TE are shown in Fig. 7. Elution occurred between 1.2 and 2.8 BV for REE and 1.2 to 4.5 for TE. Elution profile of TE, showed peaks with a maximum centred over 1.6 BV, indicating that the complexing properties of EDTA were not strong enough to displace the sulfonic complexing properties and no chromatographic elution effect was observed.

For TE, where the EDTA-TE complexes are weaker in many cases than for REE, some chromatographic separation effect is observed with the peak displacement for REE. In both cases, the concentration factors achieved were between 30 and 40 depending of the REE nature (see breakthrough splitting behaviour in Fig. 6). It could be observed that values of 510 mg/L were measured for Ce and 300 mg/L for La. Similar effect was observed for TE, however, since they were not removed effectively, their presence is reduced in terms of molar ratio to REE.

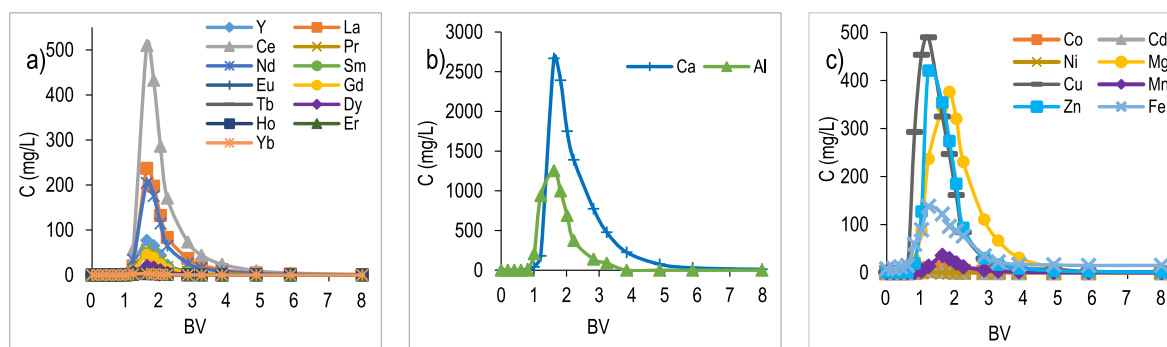The improvement of the resins performance in terms of achieving

Fig. 7. Elution curves showing the variation of the metal ions concentrations using 0.5 Na_2-EDTA and 1M NH_4Cl for: a) REEs, b) Al, Ca and c) TEs in BV for SPC11 resin.
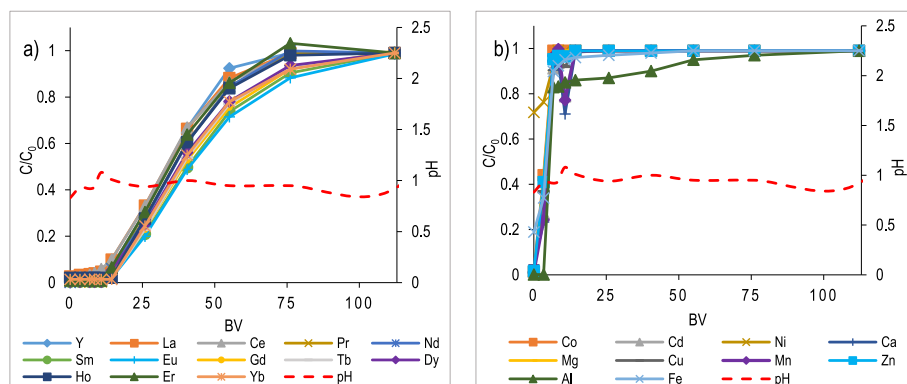
Fig. 8. Breakthrough curves (C/C$_0$) and the evolution of the acidity at the column effluent as a function of the treated solution in BV for a) REE, b) TE and the evolution in acidity (dashed line) at the column effluent as a function of the TAMW solution in BV for S957 resin.
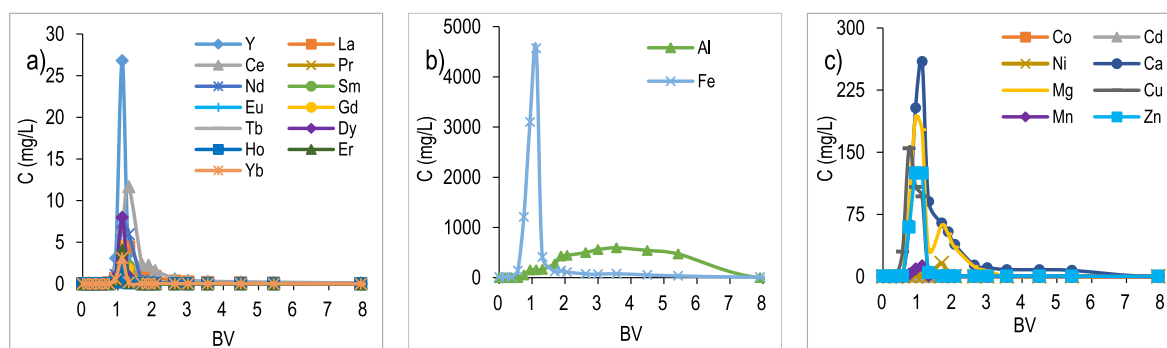

Fig. 9. Elution curves showing the variation of the metal ions concentrations using 0.5 Na$_2$-EDTA and 1M NH$_4$Cl for: a) REEs, b) Fe and Al and c) TEs in BV for S957 resin.

higher breakthrough curves should be directed to reduce the presence of major interfering ions as Al(III), Ca(II) and Mg(II) as the increase of the resins capacity is an effort under development by some resins manufacturers. The removal of Al(III) in the pre-treatment stage could be increase however it could be connected to undesired removal of REE what could affect the economic feasibility of the recovery process.

3.5.2. Concentration of REE with S957 using TAMW acidified at pH 2

Breakthrough curves for concentration of REE in TAMW with pH adjusted to 2 are depicted in Fig. 8a, taking C/C$_0$ (0.10) as breakthrough point, reported values between 20 and 25 for REE with similar profiles for both LREE and HREE contrary to the observed selectivity trends in batch experiments. At the acidity conditions used, most TE were mobilized at 15 BV with the only exception of Al which was partially retained up until 75 BV as shown in Fig. 8b.

Under such conditions S957 is shown as a good candidate for the separation of REE from TE under acidic conditions with pH values below 2. The pH has decreased at the beginning of the experiment from 2 to 1, due to the reaction of metals with the resin, as was postulated by Eqs. (4)–(6). At the end of the experiment, when the saturation of the resin has been reached, the pH of the effluent equals that of the influent.

When comparing the performance of SPC11, with a sulphonic group, in terms of resin capacity with S957 with a mixture of a sulphonic and phosphonic group, it is clearly pointed put its high performance with higher breakthrough values for REE (up to 5 times higher). Even it is possible to postulate a two-column configuration where the first column is kept until reaching total saturation of the resin capacity and the second one is stopped at the breakthrough point, By using this operation approach the resins capacity could be increase of a factor of 7, as C/C$_0$ values for SPC11 are reached at 700 BV while for S957are reached at after 100 BV.

Results on elution performance of the column after treating 115 BV using 0.5 M Na$_2$-EDTA and 1 M NH$_4$Cl are shown on Fig. 9. Elution profiles showed a sharp peak with less than 0.5 BV which allows obtaining concentration factors of up to 20 to 30 times. A small displacement for LREE is observed. Peaks centre displacements are due to the complexing properties of REEs with EDTA, the smaller the complexing constant earlier is the elution peak. More than 95% of TE were eluted in less 1 BV including trivalent elements (Fe(III) and Al. Elution profiles of TE also showed sharp peaks with some maximum displacement indicating the efficiency of the elution step, and the influence of the complexing properties of the sulfonic and phosphonic groups with the EDTA-TE complexes. As example, Fe(III) forming stronger complexes with EDTA is eluted first.

Finally, the resulting REE-enriched solution can be treated with precipitating agents, such as oxalic acid to produce a concentrate of REE oxides by calcination (Zhang et al., 2020). the sustainability of the process will be linked to the need of recovering the excess of elution solution. The integration of acid resistance nanofiltration (NF) membranes to up to 20–50% H$_2$SO$_4$ solutions will provide the possibility to recover the H$_2$SO$_4$ excess and at the same time to provide a second concentration factor for the REEs as those are rejected by the NF membrane (López et al., 2018, 2021a). The valorisation of the eluted REE from elution concentrates could integrate NF to recover up-to 90% of the free sulfuric solution present.

The screening stage developed with the three resins selected two monofunctional containing a sulphonic group and an aminophosphonic group and one bifunctional resins containing a mixture of sulphonic and phosphinic groups shown promising results for the potential recovery of REE from AMW. The low contents of REE in the AMW directed the integration of the IX resins after a simplest pre-treatment of Fe(II) removal as it is the main cation in solution. Preliminary results of the

screening stage shown that not removed species as Al(III) and major transition elements as Ca (II) and Mg(II) are reducing resins capacity for REE. However, removal and recovery efficiencies measured for REE are promising results to extent the research in this direction. It is also clearly shown that the target separation of REE from TE and post transition elements is the only objective that could be achieved. As the use of sulfuric acid as regenerant solution is also providing high performance and then as the objective is not developing any potential separation of REE in families (HREE ad LREE) its use in front of EDTA is also recommended.

4. Summary and conclusions

This study provides new data in the recovery of REE from secondary resources as AMW using three different IX resins characterized for performance under moderate acidity and sulfate concentration conditions. It was found that a primary Fe(III) removal step is required to enhance REE separation from AMW and reduce losses, where TAMW suitable for REE recovery can be created by addition of alkali to adjust pH close to 3.9 but below 4.0 to prevent co-precipitation of REE with Al. This removes up to 99% of Fe(III) in AMW by precipitation of schwertmannite. Quantitative removal of Al(III) (>99%), will imply the increase of pH above 6, and then the co-precipitation of most of the REE up to values of 30–40%. The associated losses of REE will limit the economic feasibility of the recovery process.

Acidity has a greater impact on the recovery of REE by ion exchange materials than sulfate ions which have previously been reported as important for REE recovery efficiency. This was observed as an increased performance of the three resins with lower pH. A suitable pH acidity-window is reached by adjusting pH of TAMW to values below 2 with sulfuric acid. This reduction of pH affects the removal extraction ratios for TE, especially for divalent metal ions. Trivalent metal ions are still efficiently extracted at acidic pH values with the exception Al. A suitable pH range for extraction of REE from TAMW is in the range of pH 0.5–2.0.

The mono-functional sulfonic resins provide the best selectivity factors for the extraction of REE compared to aminophosphonic and sulfonic/phosponic resins evaluated in the present work. The combination of sulfonic and phosphonic performed better than the monofunctional aminophosphonic resins, as displayed by higher kinetic performance and by higher selectivity for REE. Elution using an acid cycle (H_2SO_4) was effective and provided column regeneration cycles with 1–2 BVs, especially for the sulfonic and bifunctional sulfonic/phosphonic resins whereas the aminophosphonic resin displayed the highest BV of elution solution. For this reason, only resins with sulfonic groups should be considered for further REE concentration using EDTA treatment. The greatest concentration factors observed in the present, up to a factor of 260 for La and 160 for Ce, were achieved when the extraction stage was carried out at pH between 0.5 and 2.0 using 0.5 M Na_2EDTA/ 1 M NH_4Cl solution and a mono-functional sulfonic resin.

CRediT authorship contribution statement

M. Hermassi: Conceptualization, Data curation, Formal analysis, Writing – original draft, Formal analysis. **M. Granados:** Conceptualization, Funding acquisition, Writing – review & editing. **C. Valderrama:** Conceptualization, Funding acquisition, Writing – review & editing. **N. Skoglund:** Conceptualization, Funding acquisition, Writing – review & editing. **C. Ayora:** Conceptualization, Funding acquisition, Writing – review & editing, and. **J.L. Cortina:** Conceptualization, Funding acquisition, Resources, Supervision, Writing – review & editing.

Declaration of competing interest

The authors declare that they have no known competing financial interests or personal relationships that could have appeared to influence

the work reported in this paper.

Data availability

Data will be made available on request.

Appendix A. Supplementary data

Supplementary data to this article can be found online at https://doi.org/10.1016/j.jclepro.2022.134742.

References

Ang, K.L., Li, D., Nikoloski, A.N., 2017. The effectiveness of ion exchange resins in separating uranium and thorium from rare earth elements in acidic aqueous sulfate media. Part 1. Anionic and cationic resins. Hydrometallurgy 174, 147–155.

Ayora, C., Caraballo, M.A., Macias, F., Rotting, T.S., Carrera, J., Nieto, J.M., 2013. Acid mine drainage in the Iberian Pyrite Belt: 2. Lessons learned from recent passive remediation experiences. Environ. Sci. Pollut. Res. Int. 20 (11), 7837–7853.

Ayora, C., Macias, F., Torres, E., Lozano, A., Carrero, S., Nieto, J.M., Perez-Lopez, R., Fernandez-Martinez, A., Castillo-Michel, H., 2016. Recovery of rare earth elements and yttrium from passive-remediation systems of acid mine drainage. Environ. Sci. Technol. 50 (15), 8255–8262.

Bigham, J.M., Schwertmann, U., Traina, S.J., Winland, R.L., Wolf, M., 1996. Schwertmannite and the chemical modeling of iron in acid sulfate waters. Geochem. Cosmochim. Acta 60 (12), 2111–2121.

Callura, J.C., Shi, Q., Dzombak, D.A., Karamalidis, A.K., 2021. Selective recovery of rare earth elements with ligand-functionalized polymers in fixed-bed adsorption columns. Separ. Purif. Technol. 265.

Chen, Z., 2011. Global rare earth resources and scenarios of future rare earth industry. J. Rare Earths 29 (1), 1–6.

COM, 2020. Critical raw materials resilience: charting a path towards greater security and sustainability. Brussels 3.9, 2020 COM 474 final.

Crittenden, John C., R.T., R., Hand, David W., Howe, Kerry J., George, Tchobanoglous, 2012. MWH's Water Treatment_ Principles and Design, third ed. John Wiley & Sons.

Diallo, M.S., Kotte, M.R., Cho, M., 2015. Mining critical metals and elements from seawater: opportunities and challenges. Environ. Sci. Technol. 49 (16), 9390–9399.

DOE, 2011. Department of Energy, p. 188. Critical Materials Strategy DOE/PI-0009.

Fritz, A.G., Tarka, T.J., Mauter, M.S., 2021. Technoeconomic assessment of a sequential step-leaching process for rare earth element extraction from acid mine drainage precipitates. ACS Sustain. Chem. Eng. 9 (28), 9308–9316.

Hamza, M.F., Wei, Y., Khalafalla, M.S., Abed, N.S., Fouda, A., Elwakeel, K.Z., Guibal, E., Hamad, N.A., 2022. U(VI) and Th(IV) recovery using silica beads functionalized with urea- or thiourea-based polymers - application to ore leachate. Sci. Total Environ. 821, 153184.

He, C., Salih, K.A.M., Wei, Y., Mira, H., Abdel-Rahman, A.A.H., Elwakeel, K.Z., Hamza, M.F., Guibal, E., 2021. Efficient recovery of rare earth elements (Pr(III) and Tm(III)) from mining residues using a new phosphorylated hydrogel (algal Biomass/ PEI). Metals 11 (2).

Hedin, B.C., Capo, R.C., Stewart, B.W., Hedin, R.S., Lopano, C.L., Stuckman, M.Y., 2019. The evaluation of critical rare earth element (REE) enriched treatment solids from coal mine drainage passive treatment systems. Int. J. Coal Geol. 208, 54–64.

Hermassi, M., Granados, M., Valderrama, C., Ayora, C., Cortina, J.L., 2021a. Recovery of Rare Earth Elements from acidic mine waters by integration of a selective chelating ion-exchanger and a solvent impregnated resin. J. Environ. Chem. Eng. 9 (5).

Hermassi, M., Granados, M., Valderrama, C., Ayora, C., Cortina, J.L., 2021b. Recovery of rare earth elements from acidic mine waters: an unknown secondary resource. Sci. Total Environ. 810, 152258.

Izatt, R.M., Izatt, S.R., Bruening, R.L., Izatt, N.E., Moyer, B.A., 2014. Challenges to achievement of metal sustainability in our high-tech society. Chem. Soc. Rev. 43 (8), 2451–2475.

Jha, M.K., Kumari, A., Panda, R., Rajesh Kumar, J., Yoo, K., Lee, J.Y., 2016. Review on hydrometallurgical recovery of rare earth metals. Hydrometallurgy 161.

Kertman, S.V., Kertman, G.M., Leykin, Y.A., 1995. A thermochemical study of complex formation in chelating ion-exchange resins. Thermochim. Acta 256, 227–235.

Kuz'min, V.I., Kuz'min, D.V., 2014. Sorption of nickel and copper from leach pulps of low-grade sulfide ores using Purolite S930 chelating resin. Hydrometallurgy 141, 76–81.

Larochelle, T., Noble, A., Ziemkiewicz, P., Hoffman, D., Constant, J., 2021. A fundamental economic assessment of recovering rare earth elements and critical minerals from acid mine drainage using a network sourcing strategy. Minerals 11 (11).

Littlejohn, P., Vaughan, J., 2012. Selectivity of commercial and novel mixed functionality cation exchange resins in mildly acidic sulfate and mixed sulfate–chloride solution. Hydrometallurgy 121–124, 90–99.

López, J., Reig, M., Gibert, O., Torres, E., Ayora, C., Cortina, J.L., 2018. Application of nanofiltration for acidic waters containing rare earth elements: influence of transition elements, acidity and membrane stability. Desalination 430, 33–44.

López, J., Gibert, O., Cortina, J.L., 2021a. Integration of membrane technologies to enhance the sustainability in the treatment of metal-containing acidic liquid wastes. An overview. Separ. Purific. Technol. 265.

López, J., Reig, M., Vecino, X., Cortina, J.L., 2021b. Arsenic impact on the valorisation schemes of acidic mine waters of the Iberian Pyrite Belt: integration of selective precipitation and spiral-wound nanofiltration processes. J. Hazard Mater. 403.

Lozano, A., Ayora, C., Fernández-Martínez, A., 2019. Sorption of rare earth elements onto basaluminite: the role of sulfate and pH. Geochem. Cosmochim. Acta 258, 50–62.

Lozano, A., Ayora, C., Fernández-Martínez, A., 2020. Sorption of rare earth elements on schwertmannite and their mobility in acid mine drainage treatments. Appl. Geochem. 113.

Massari, S., Ruberti, M., 2013. Rare earth elements as critical raw materials: focus on international markets and future strategies. Resour. Pol. 38 (1), 36–43.

McKevitt, B., Dreisinger, D., 2009a. A comparison of various ion exchange resins for the removal of ferric ions from copper electrowinning electrolyte solutions part I: electrolytes containing no other impurities. Hydrometallurgy 98 (1–2), 116–121.

McKevitt, B., Dreisinger, D., 2009b. A comparison of various ion exchange resins for the removal of ferric ions from copper electrowinning electrolyte solutions Part II: electrolytes containing antimony and bismuth. Hydrometallurgy 98 (1–2), 122–127.

Mirjalili, K., Roshani, M., 2007. Resin-in-pulp method for uranium recovery from leached pulp of low grade uranium ore. Hydrometallurgy 85 (2–4), 103–109.

Nieto, J.M., Sarmiento, A.M., Canovas, C.R., Olias, M., Ayora, C., 2013. Acid mine drainage in the Iberian Pyrite Belt: 1. Hydrochemical characteristics and pollutant load of the Tinto and Odiel rivers. Environ. Sci. Pollut. Res. Int. 20 (11), 7509–7519.

Noack, C.W., Dzombak, D.A., Karamalidis, A.K., 2014. Rare earth element distributions and trends in natural waters with a focus on groundwater. Environ. Sci. Technol. 48 (8), 4317–4326.

Opare, E.O., Struhs, E., Mirkouei, A., 2021. A comparative state-of-technology review and future directions for rare earth element separation. Renew. Sustain. Energy Rev. 143.

Page, M.J., Soldenhoff, K., Ogden, M.D., 2017. Comparative study of the application of chelating resins for rare earth recovery. Hydrometallurgy 169, 275–281.

Page, M.J., Quinn, J.E., Soldenhoff, K.H., 2019. The impact of sulfate ions on the ion exchange of rare earth elements. Hydrometallurgy 186, 12–20.

Papangelakis, V.G., Moldoveanu, G., 2014. Recovery of rare earth elements from clay minerals, ERES 2014: 1st European Rare Earth Resources Conference. In: 1st European Rare Earth Resources Conference|Milos|04–07/09/2014.

Quinn, J.E., Soldenhoff, K.H., Stevens, G.W., Lengkeek, N.A., 2015. Solvent extraction of rare earth elements using phosphonic/phosphinic acid mixtures. Hydrometallurgy 157, 298–305.

Radhika, S., Nagaraju, V., Nagaphani Kumar, B., Kantam, M.L., Reddy, B.R., 2012. Solid-liquid extraction of Gd(III) and separation possibilities of rare earths from phosphoric acid solutions using Tulsion CH-93 and Tulsion CH-90 resins. J. Rare Earths 30 (12), 1270–1275.

Reddy, B.R., Kumar, J.R., 2016. Rare earths extraction, separation, and recovery from phosphoric acid media. Solvent Extr. Ion Exch. 34 (3), 226–240.

Reig, M., Vecino, X., Hermassi, M., Valderrama, C., Gibert, O., Cortina, J.L., 2019. Integration of selectrodialysis and solvent-impregnated resins for Zn(II) and Cu(II) recovery from hydrometallurgy effluents containing As(V). Separ. Purif. Technol. 229.

Silva, R.A., Hawboldt, K., Zhang, Y., 2018. Application of resins with functional groups in the separation of metal ions/species – a review. Miner. Process. Extr. Metall. Rev. 39 (6), 395–413.

Simate, G.S., Ndlovu, S., 2014. Acid mine drainage: challenges and opportunities. J. Environ. Chem. Eng. 2 (3), 1785–1803.

Sole, K.C., 2008. Solvent extraction in the hydrometallurgical processing and purification of metals: process design and selected applications. In: Aguilar, M., Cortina, J.L. (Eds.), Solvent Extraction and Liquid Membranes: Fundamentals and Applications in New Materials. Taylor & Francis. CRC Press, Boca Raton, pp. 141–200.

Stewart, B.W., Capo, R.C., Hedin, B.C., Hedin, R.S., 2017. Rare earth element resources in coal mine drainage and treatment precipitates in the Appalachian Basin, USA. Int. J. Coal Geol. 169, 28–39.

Syed, S., 2012. Recovery of gold from secondary sources—a review. Hydrometallurgy 115–116, 30–51.

Wang, Y., Ziemkiewicz, P., Noble, A., 2022. A hybrid experimental and theoretical approach to optimize recovery of rare earth elements from acid mine drainage precipitates by oxalic acid precipitation. Minerals 12 (2).

Wei, Y., Salih, K.A.M., Hamza, M.F., Rodríguez Castellón, E., Guibal, E., 2021a. Novel phosphonate-functionalized composite sorbent for the recovery of lanthanum(III) and terbium(III) from synthetic solutions and ore leachate. Chem. Eng. J. 424.

Wei, Y., Salih, K.A.M., Rabie, K., Elwakeel, K.Z., Zayed, Y.E., Hamza, M.F., Guibal, E., 2021b. Development of phosphoryl-functionalized algal-PEI beads for the sorption of Nd(III) and Mo(VI) from aqueous solutions – application for rare earth recovery from acid leachates. Chem. Eng. J. 412.

Xie, F., Zhang, T.A., Dreisinger, D., Doyle, F., 2014. A critical review on solvent extraction of rare earths from aqueous solutions. Miner. Eng. 56, 10–28.

Xiong, C., Meng, Y., Yao, C., Shen, C., 2009. Adsorption of erbium(III) on D113-III resin from aqueous solutions: batch and column studies. J. Rare Earths 27 (6), 923–931.

Xiong, C., Zhu, J., Shen, C., Chen, Q., 2012. Adsorption and desorption of praseodymium (III) from aqueous solution using D72 resin. Chin. J. Chem. Eng. 20 (5), 823–830.

Yang, X.J., Lin, A., Li, X.-L., Wu, Y., Zhou, W., Chen, Z., 2013. China's ion-adsorption rare earth resources, mining consequences and preservation. Environ. Develop. 8, 131–136.

Zhang, W., Honaker, R.Q., 2018. Rare earth elements recovery using staged precipitation from a leachate generated from coarse coal refuse. Int. J. Coal Geol. 195, 189–199.

Zhang, K., Kleit, A.N., Nieto, A., 2017. An economics strategy for criticality – application to rare earth element Yttrium in new lighting technology and its sustainable availability. Renew. Sustain. Energy Rev. 77, 899–915.

Zhang, W., Noble, A., Yang, X., Honaker, R., 2020. A comprehensive review of rare earth elements recovery from coal-related materials. Minerals 10 (5).